Correlation of LANL Sferic-Array Results With VLF Data From the National Lightning Detection Network and With VHF Data From the FORTE Satellite

Abram R. Jacobson and David A. Smith
Space and Atmospheric Sciences Group
Los Alamos National Laboratory
Mail Stop D466, LANL
Los Alamos, New Mexico 87545 U.S.A

Jeremiah Harlin
Langmuir Laboratory for Atmospheric Research
New Mexico Institute of Mining and Technology
Socorro, New Mexico 87801 U.S.A.

For an electronic copy of this poster, kindly send a request to ajacobson@lanl.gov

Please visit our websites at
http://forte.lanl.gov/
and
http://nis-www.lanl.gov/nis-projects/forte_science/

FORTE has been used in a campaign mode with the Los Alamos 11-station sferic-waveform array, over two summer thunderstorm seasons (1998 and 1999). In this mode, the memory aboard FORTE is devoted to the maximum extent possible to storing waveforms collected while FORTE is within sight of the array stations' region. In turn, during FORTE visibility, those stations were run at lower trigger threshhold, so that their data-storage resources were also concentrated on periods of joint FORTE/array access to the same storms.

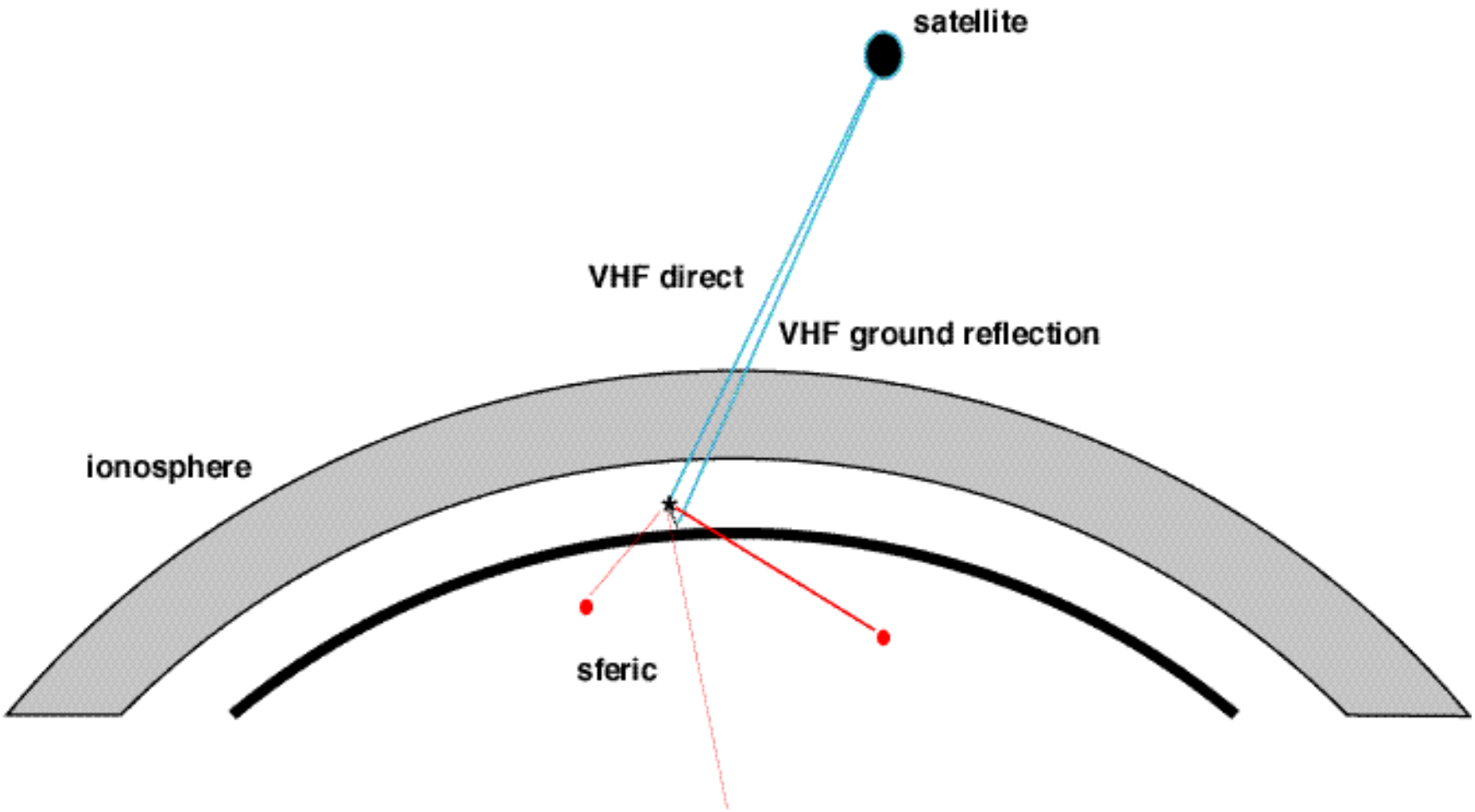

This shows a day's worth of FORTE collections connected to a very intense and prolonged storm off Florida's east coast, as well as some less-intense storms elsewhere. Altogether, five FORTE passes "saw" the storm, in the sense that FORTE VHF triggers, when corrected to the nearest sferic-array event solution, coincided with sferics to within ±5 ms. The blue diamonds are the sferic solutions, while the orange squares are the subsatellite points, for the correlations. Each correlated pair is connected by a yellow line. The most fruitful FORTE pass went almost directly over the storm.

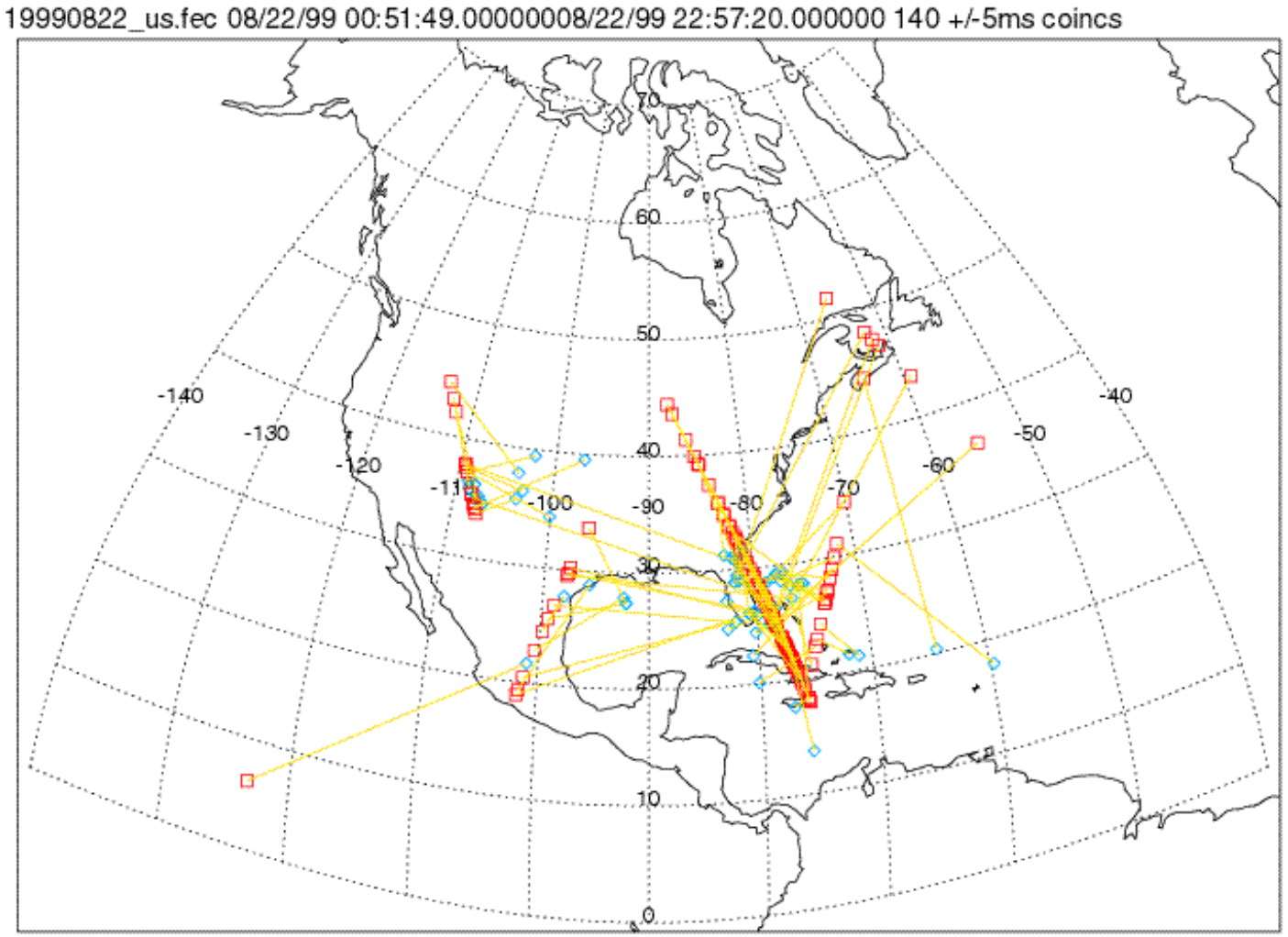

During the most fruitful FORTE pass over the Florida storm, we collected hundreds of FORTE VHF pulsed events whose inter-pulse separation and fitted slant total electron content (TEC) are shown below. This is the classic signature of FORTE flight past a recurrently emitting lightning storm. Most of the pulse separations are on a curve which is consistent with the emission centers being at roughly constant height above the reflective ocean.

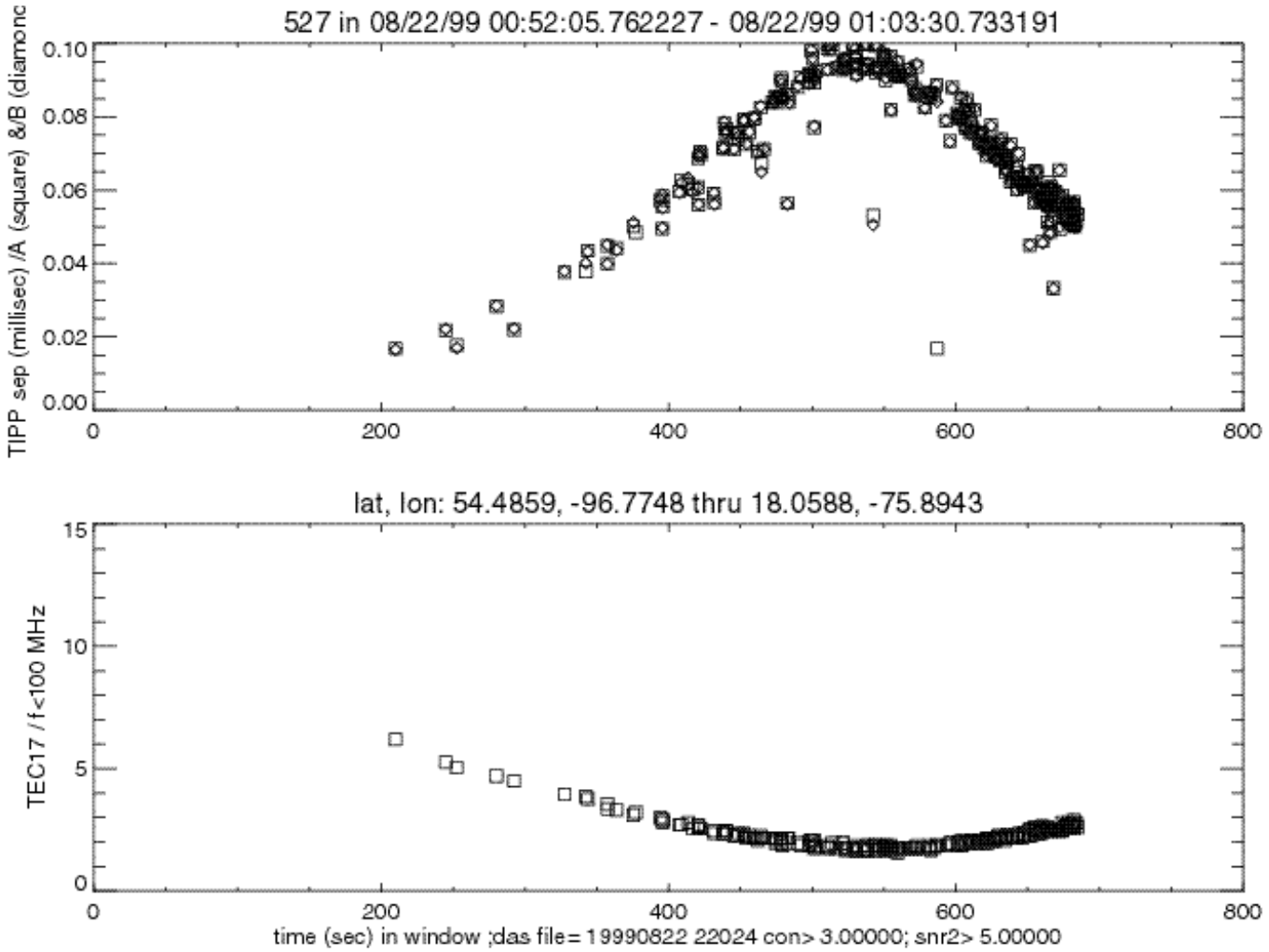

Histogram of FORTE elevation angle seen from locations of sferics, for background (dashed) and probable-coincident (solid) sferics. Apparently the liklihood of a FORTE VHF detection peaks for the satellite overhead and declines for the satellite on the horizon, a trend which is consistent both with earlier NLDN experience and triggering and antenna-lobe common sense

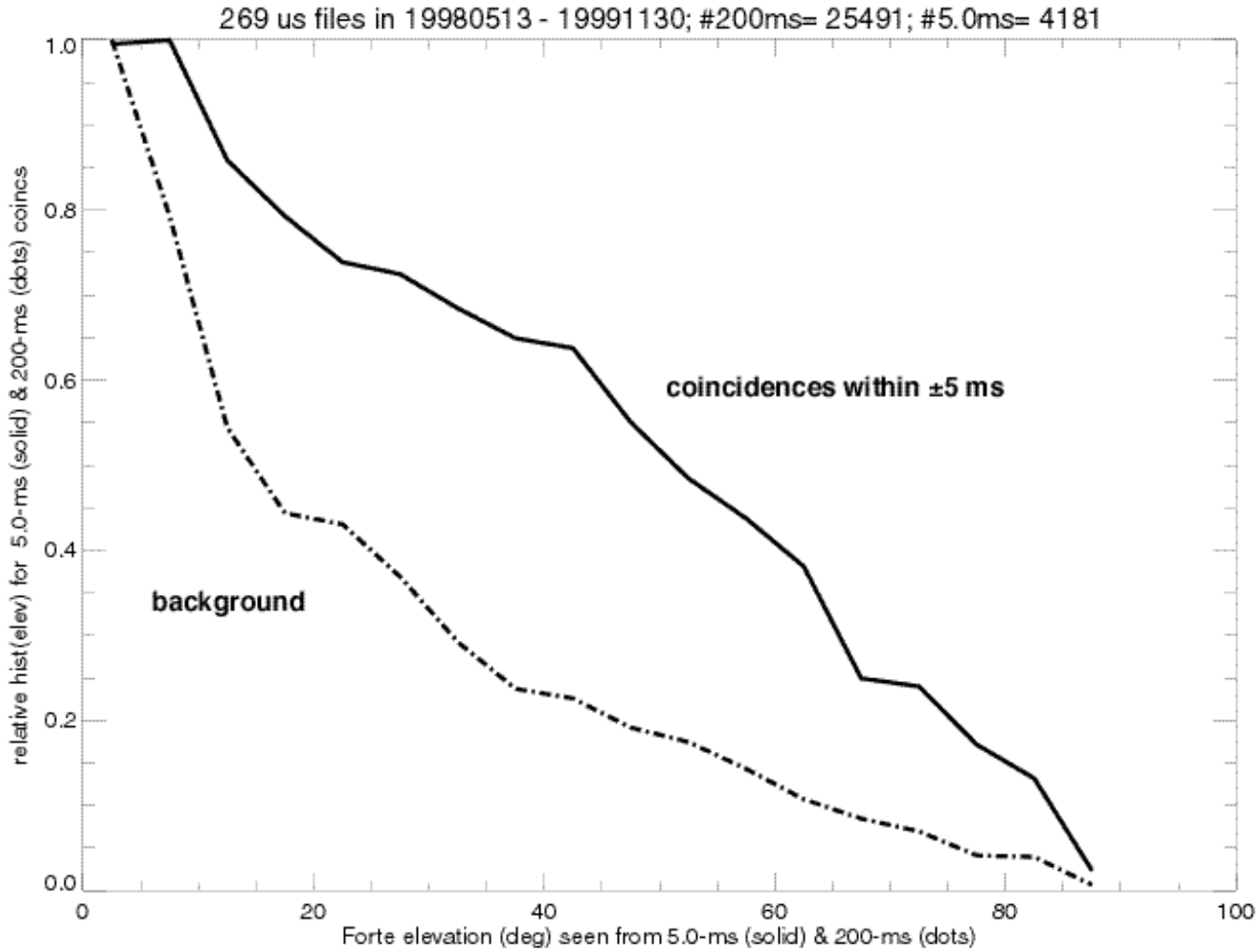

Histogram of [sferic-(FORTE VHF)] signal source times, corrected for the FORTE-to-ground propagation time through vacuum. A 0.1-ms binsize is used, and the abscissa ranges from -10 ms to +10 ms. Comparing the central peak (say, within ±0.3 ms) with the statistical-accident pedestal, we can ascribe the central peak's events as being true coincidences with >95% reliability. There is a slight enhancement in the range +1 ms to +3 ms compared to the range -1 ms to -3 ms. This corresponds to the increased incidence of VHF emission before the sferic emission, rather than after the sferic emission.

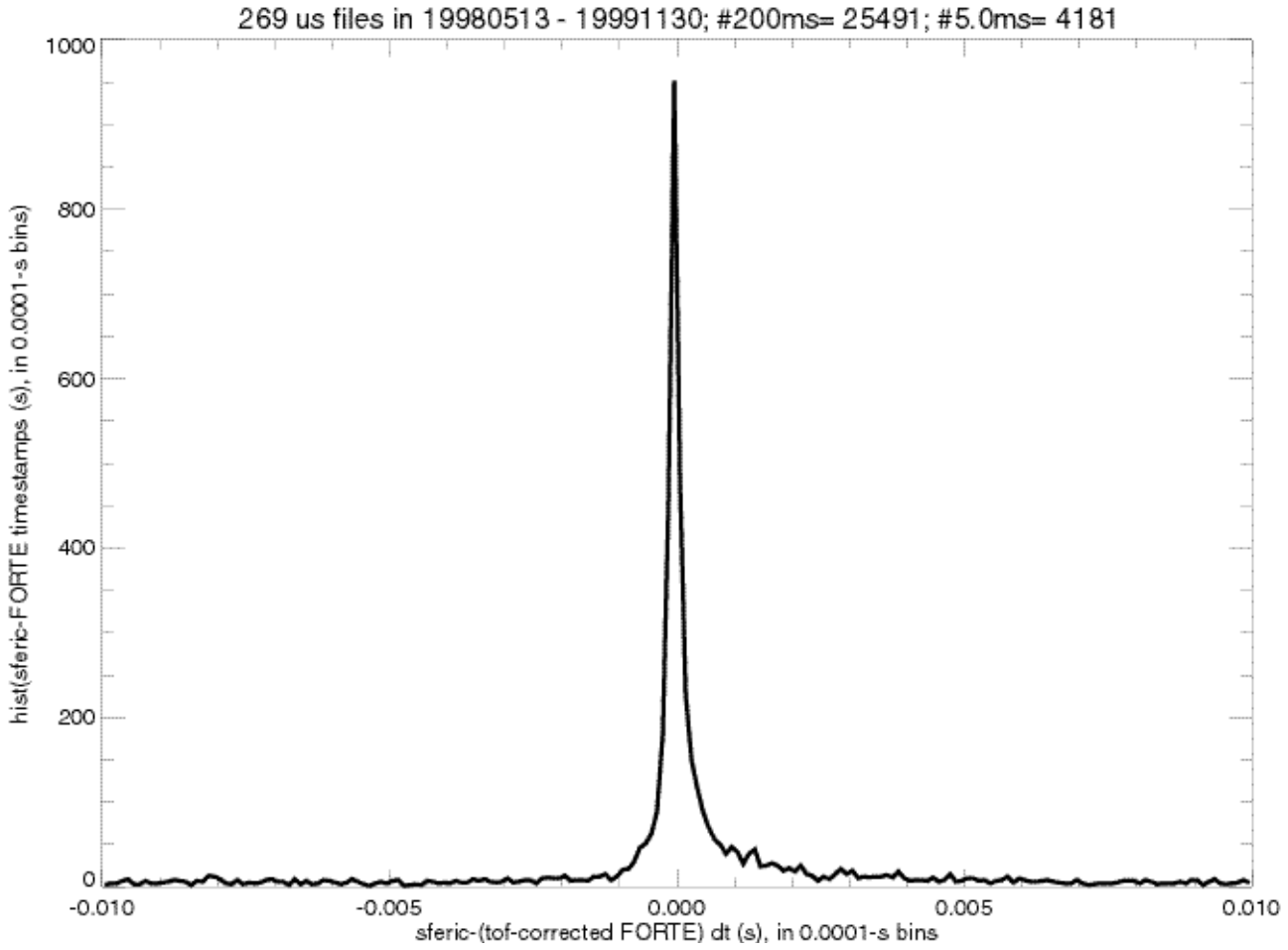

Histogram of distance from sferic emission to the third-closest sferic-detection station participating in the solution. Since the close-in array scale is on the order of ~200 km, we would prefer that the events we study not be >600 km (three array scales) from the core three stations participating in the fit. Unfortunately, with a sparse and incomplete array like this, we cannot satisfy that wish for any more than about 50% of the coincident events in this dataset. We therefore must accept probable errors from both "spoking" and ionospheric-pathing effects.

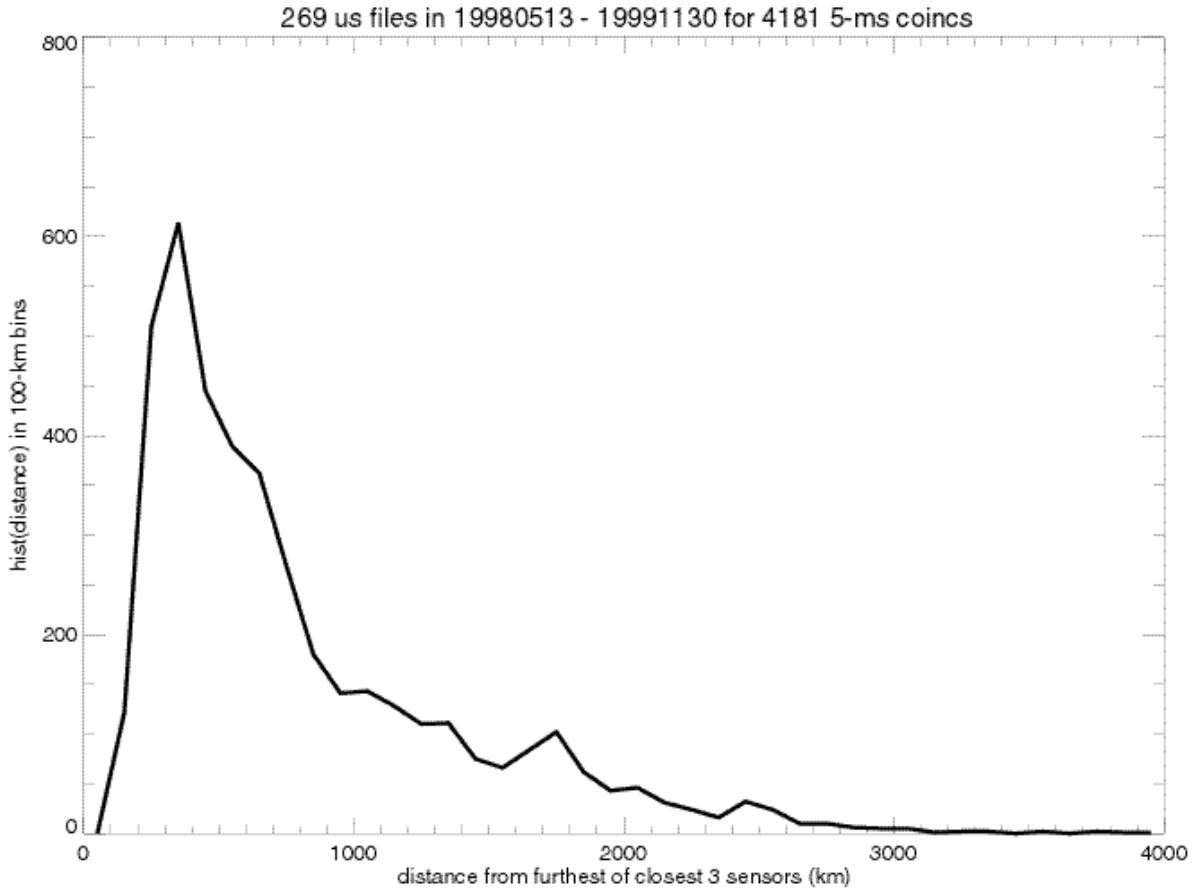

Histogram of [sferic-(FORTE VHF)] signal source times, corrected for the FORTE-to-ground propagation time through vacuum. A 0.02-ms binsize is used, and the abscissa ranges from -1 ms to +1 ms. The solid curve is for the sferics located closer than 603 km from the third-nearest station, and the dashed curve is for the sferics located further than 603 km from the third-nearest station. The distant events have a broadened and somewhat delayed (by about 0.1 ms) arrival time time of the sferic at the station, relative to the closer events.

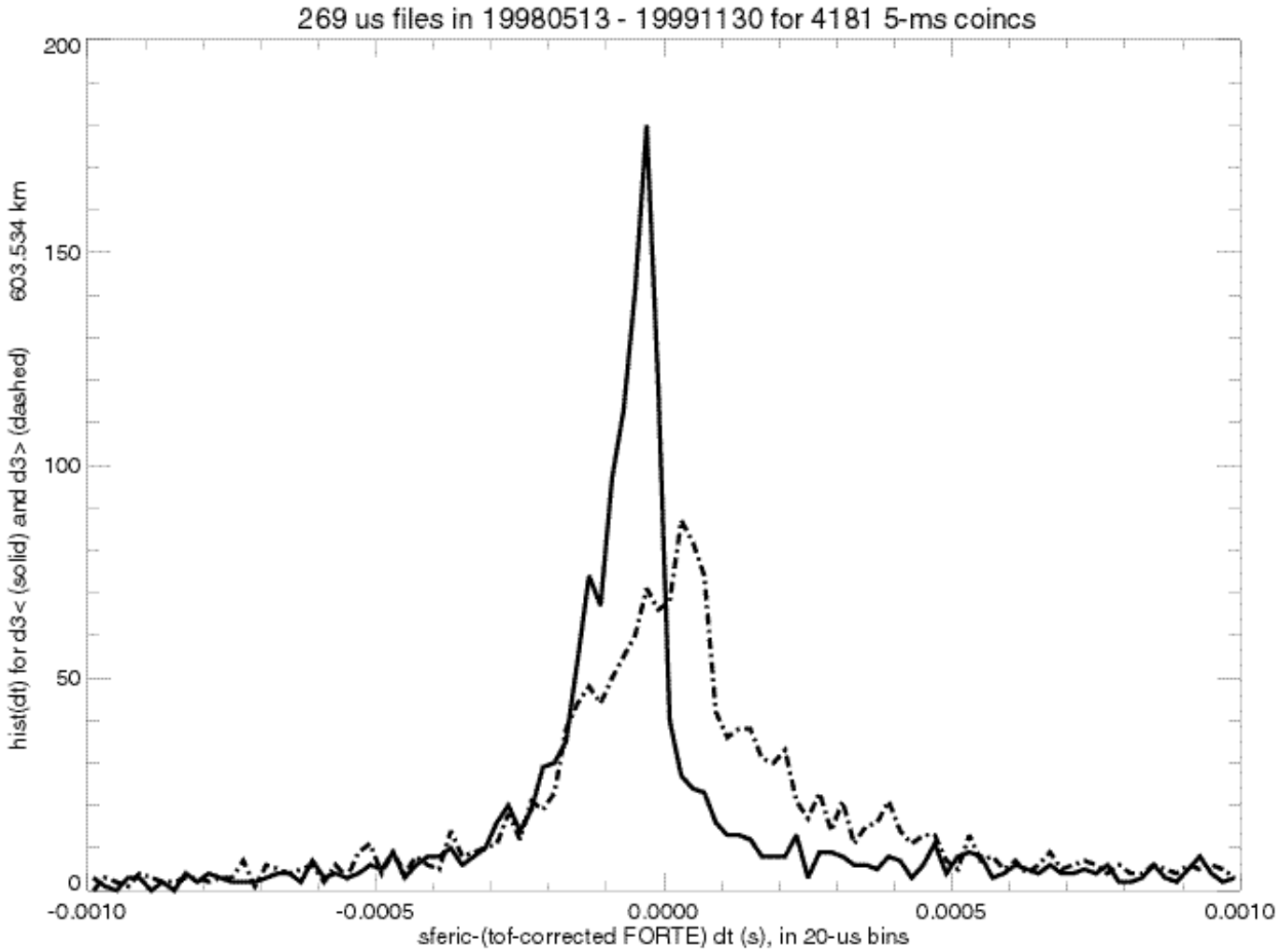

At least some of the range spread in the time-of-arrival differences could be attributed to FORTE data perturbed by a recurrent on-board data-recording problem. Restricting the sample to the 2422 coincidences for which we can prove this problem did not occur, and for which the coincidence is within ±0.3 ms, we show the revised histogram of [sferic-(FORTE VHF)] signal source times, corrected for the FORTE-to-ground time propagation time through vacuum. A 0.05-ms binsize is used, and the abscissa ranges from -1 ms to +1 ms. The solid curve is for the sferics located closer than 600 km from the third-nearest station, and the dashed curve is for the sferics located further than 600 km from the third-nearest station. Having tightened the FORTE-event-selection criteria, we have eliminated most of the range spread.

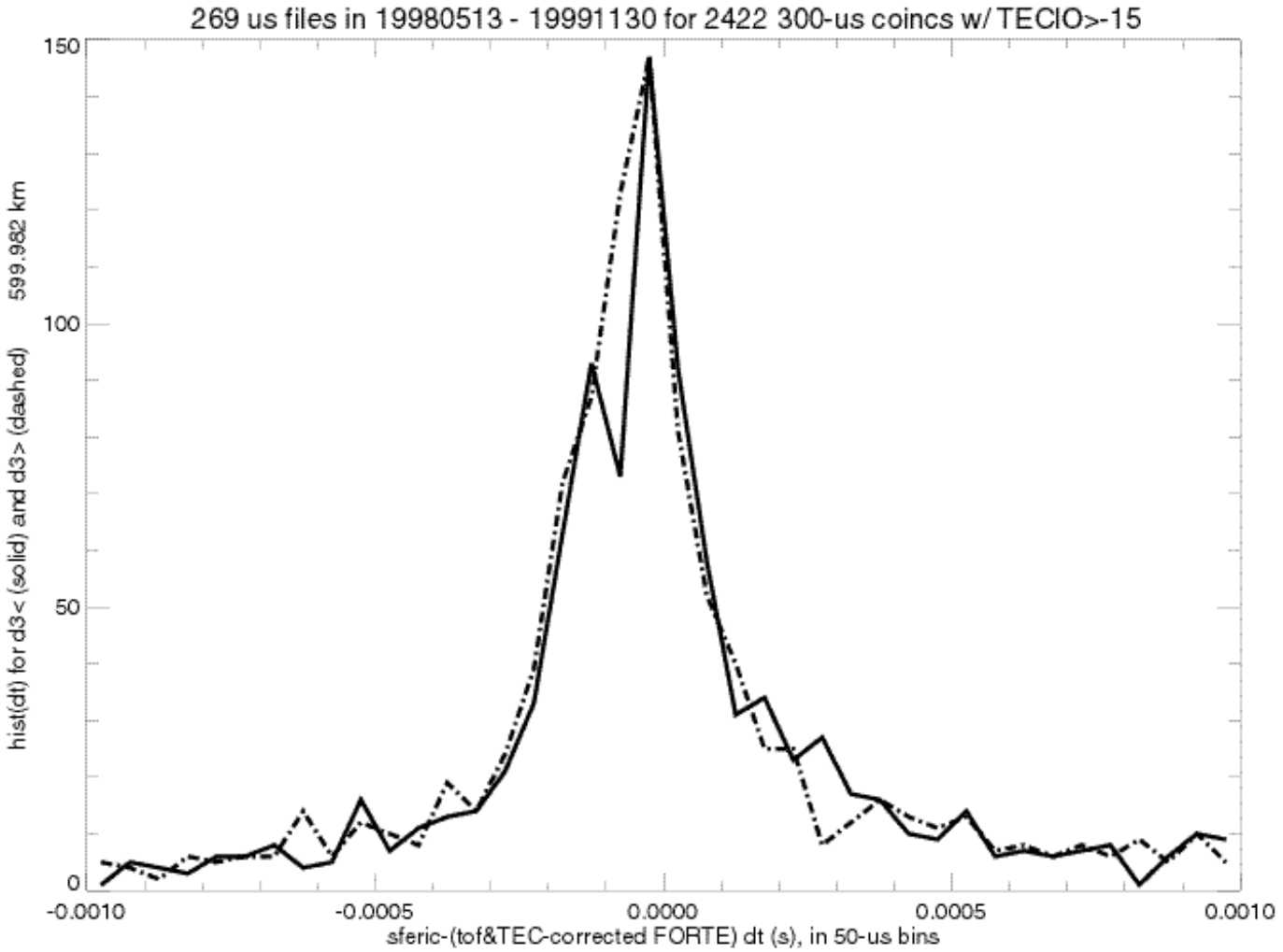

This cartoon shows the two methods for independently arriving at estimates of a signal's emission height (above the ground). The emitter (for this example, shown in yellow and co-located for both the signals) is at a known latitude and longitude; we seek the height from our data. The satellite receives a direct VHF pulse (orange) and a ground-reflected VHF pulse (pink). The time-delay of between these two pulses can furnish the emitter height, since the source's horizontal geolocation is known. The ground-based field-change meter station receives a lower-frequency (3-500 kHz) signal, which arrives at the station as a direct ray (red), an ionospheric reflection (blue), and a ground reflection + ionospheric reflection (green). The relative time delay of the latter two signals provides the information on both emission height and ionospheric-reflector height.

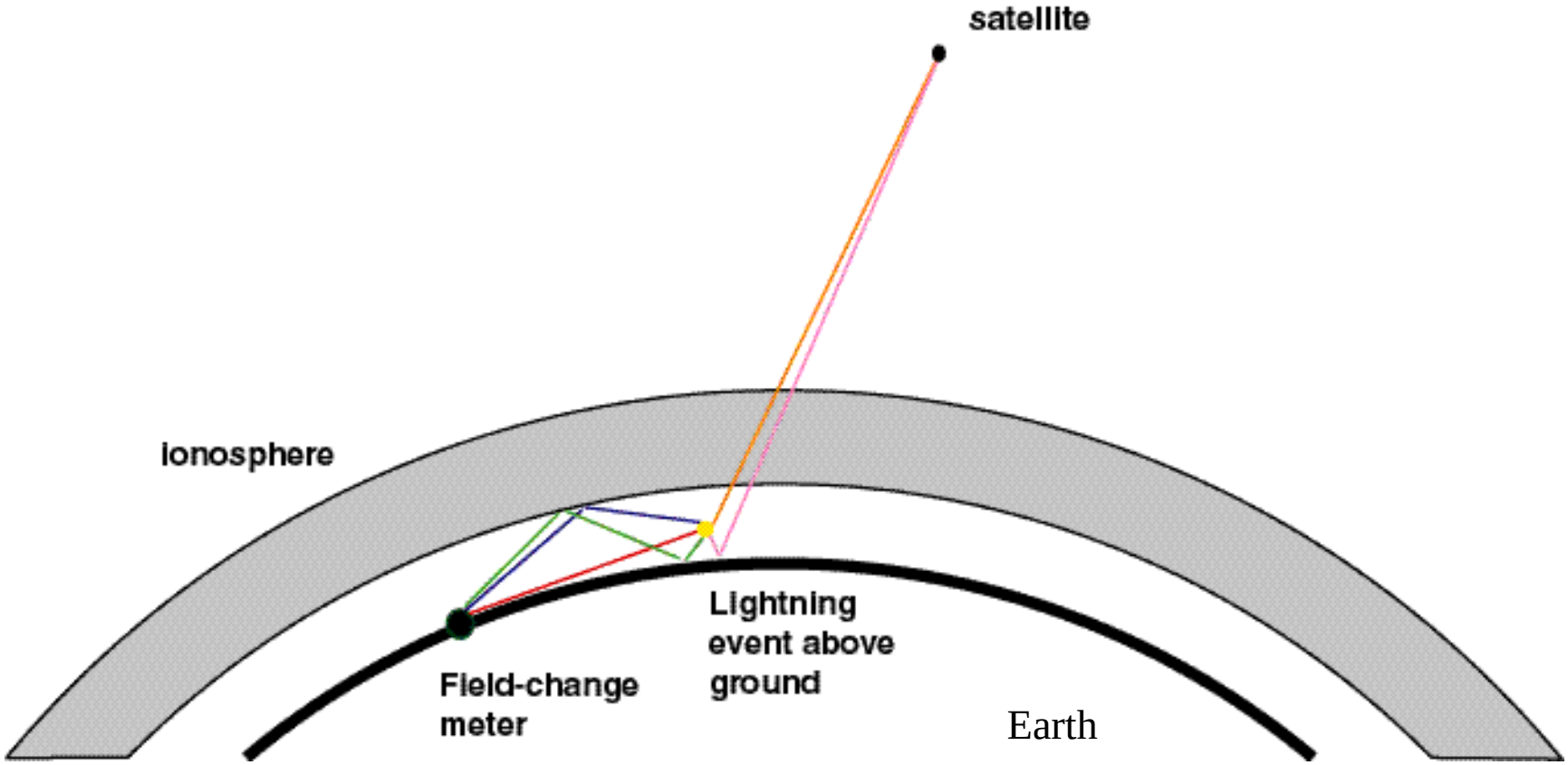

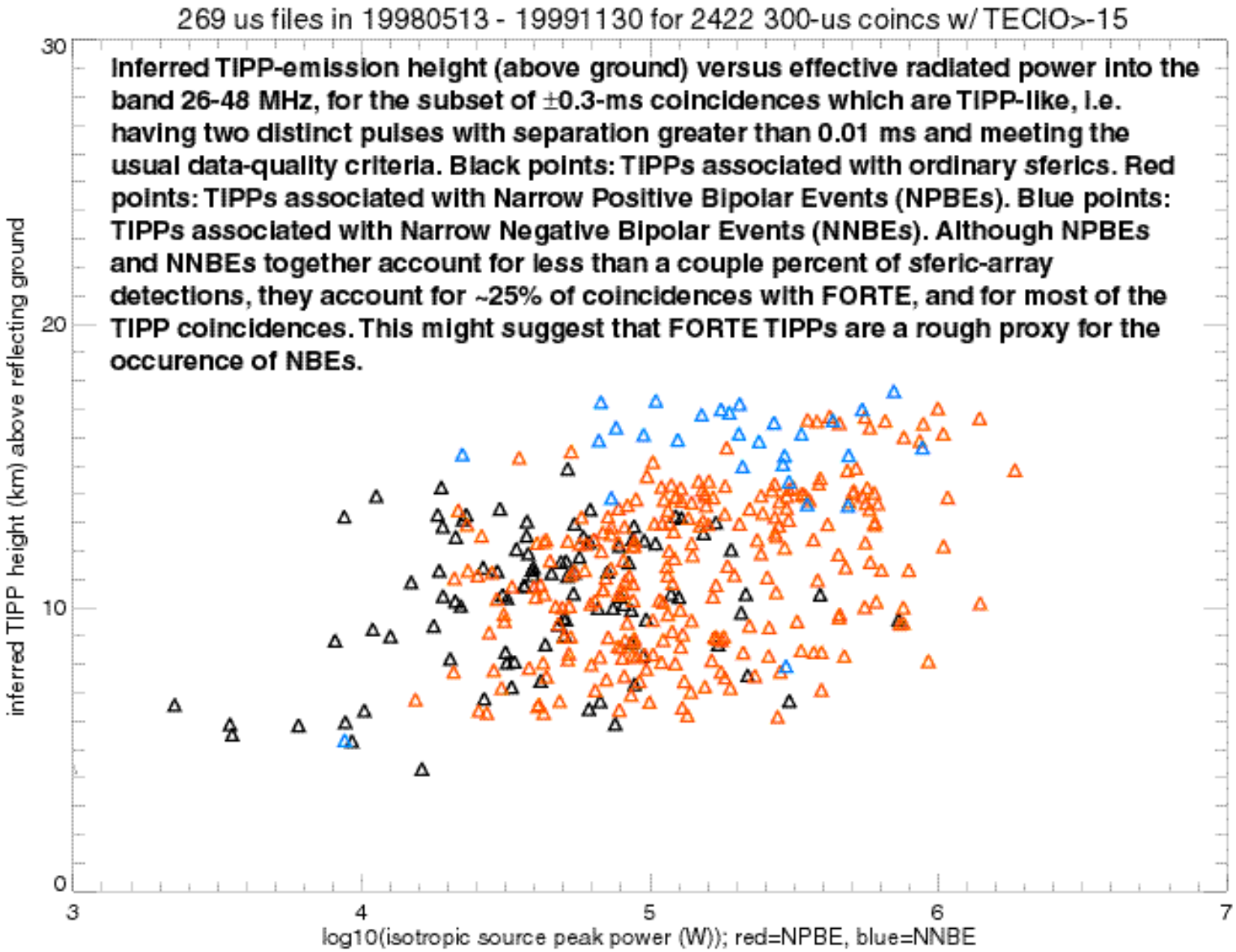
269 us files in 19980513 - 19991130 for 2422 300-us coincs w/ TECIO>-15
Inferred TIPP-emission height (above ground) versus effective radiated power into the band 26-48 MHz, for the subset of ±0.3-ms coincidences which are TIPP-like, i.e. having two distinct pulses with separation greater than 0.01 ms and meeting the usual data-quality criteria. Black points: TIPPs associated with ordinary sferics. Red points: TIPPs associated with Narrow Positive Bipolar Events (NPBEs). Blue points: TIPPs associated with Narrow Negative Bipolar Events (NNBEs). Although NPBEs and NNBEs together account for less than a couple percent of sferic-array detections, they account for ~25% of coincidences with FORTE, and for most of the TIPP coincidences. This might suggest that FORTE TIPPs are a rough proxy for the occurence of NBEs.
inferred TIPP height (km) above reflecting ground
30
20
10
0
3
4
5
6
7
log10(isotropic source peak power (W)); red=NPBE, blue=NNBE

Power-autocorrelation 1/e width vs logarithm of effective radiated power of FORTE-detected VHF pulse, in passband 26-48 MHz, for all 2422 ±0.3-ms coincidences. Black points: TIPPs associated with ordinary sferics. Red points: TIPPs associated with Narrow Positive Bipolar Events (NPBEs). Blue points: TIPPs associated with Narrow Negative Bipolar Events (NNBEs). The vast majority of VHF signatures associated with NBEs are narrow (<10 μs) and relatively powerful (>30 kW ERP into passband 26-48 MHz), compared to the VHF events coincident with non-NBE sferics.

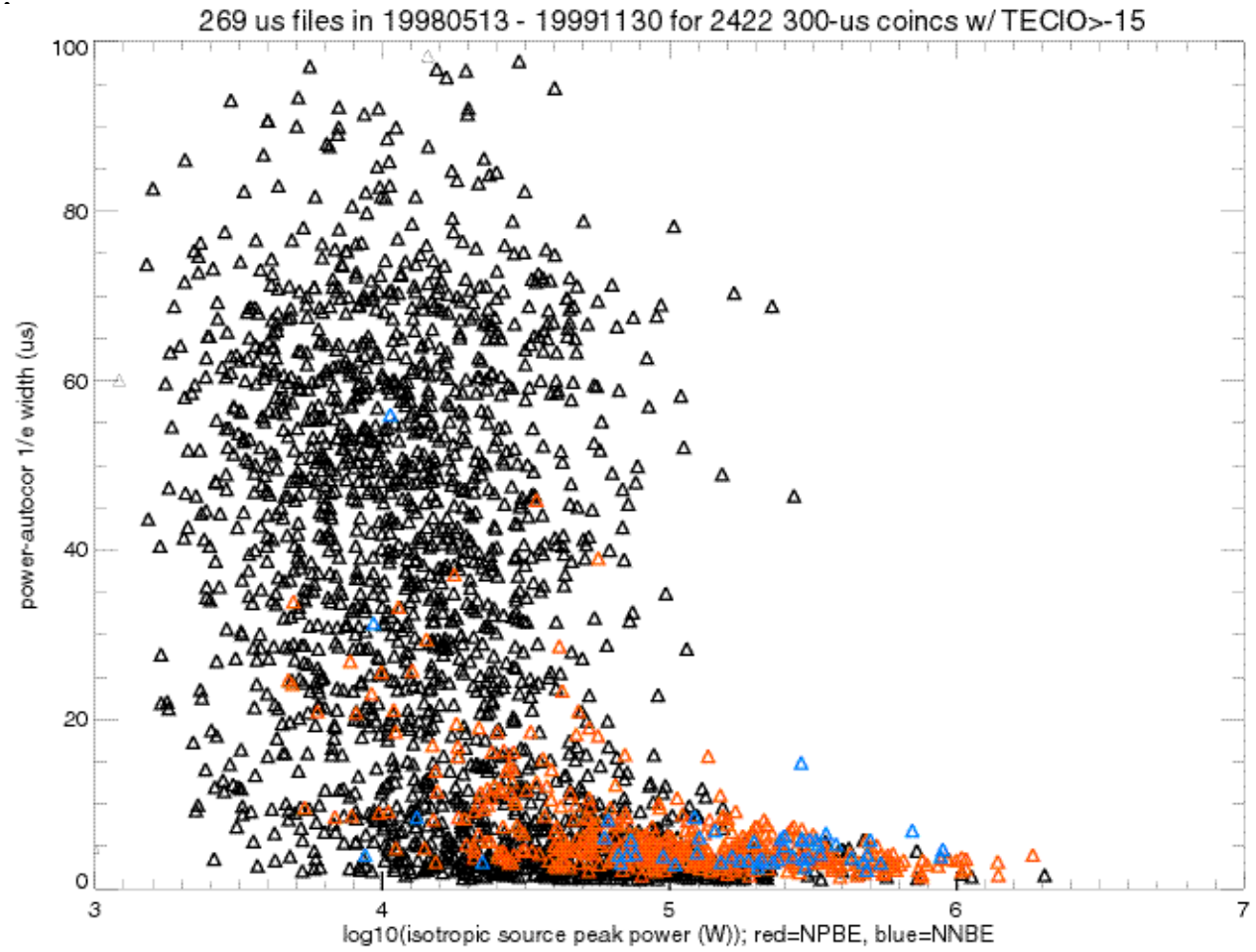

Effective energy width vs logarithm of effective radiated power of FORTE-detected VHF pulse, in passband 26-48 MHz, for all 2422 ±0.3-ms coincidences. Black points: TIPPs associated with ordinary sferics. Red points: TIPPs associated with Narrow Positive Bipolar Events (NPBEs). Blue points: TIPPs associated with Narrow Negative Bipolar Events (NNBEs). The vast majority of VHF signatures associated with NBEs are narrow (<20 μs) and relatively powerful (>30 kW ERP into passband 26-48 MHz), compared to the VHF events coincident with non-NBE sferics.

Histogram of [sferic-(FORTE VHF)] signal source times, corrected for the FORTE-to-ground propagation time through vacuum. A 0.02-ms binsize is used, and the abscissa ranges from -1 ms to +1 ms. These distributions have been corrected not only for the vacuum propagation, but also for the rf group delay traversing the ionospheric slant total electron content (TEC). Top panel: Sferic-FORTE source time differences for 1917 coincidences involving ordinary (i.e., non-NBE) sferics. Bottom panel: Sferic-FORTE source time differences for 505 coincidences involving NBEs. Note narrower distribution and sharp drop-off for VHF trailing NBE.

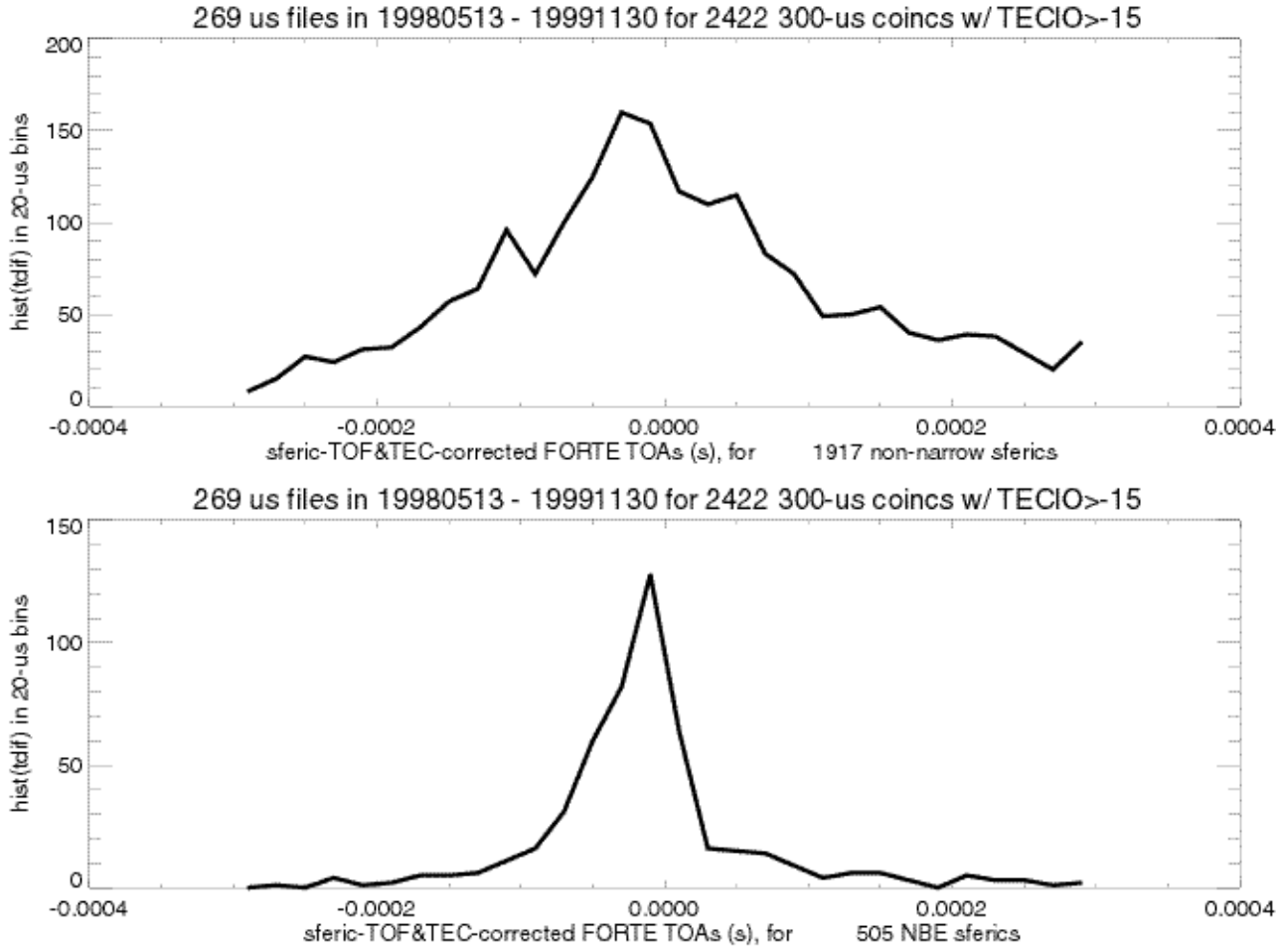

Distance to third-nearest station vs sferic-VHF source time difference. Top panel: for 1917 ordinary sferics. Bottom panel: for 505 Narrow Bipolar Events, or NBEs. The close-in NBEs (those close than ~500 km to array stations) have VHF delayed (from NBE) by typically 0 to 50 μs. This needs to be examined carefully, for it is not totally consistent with ground-based joint VHF/NBE measurements.

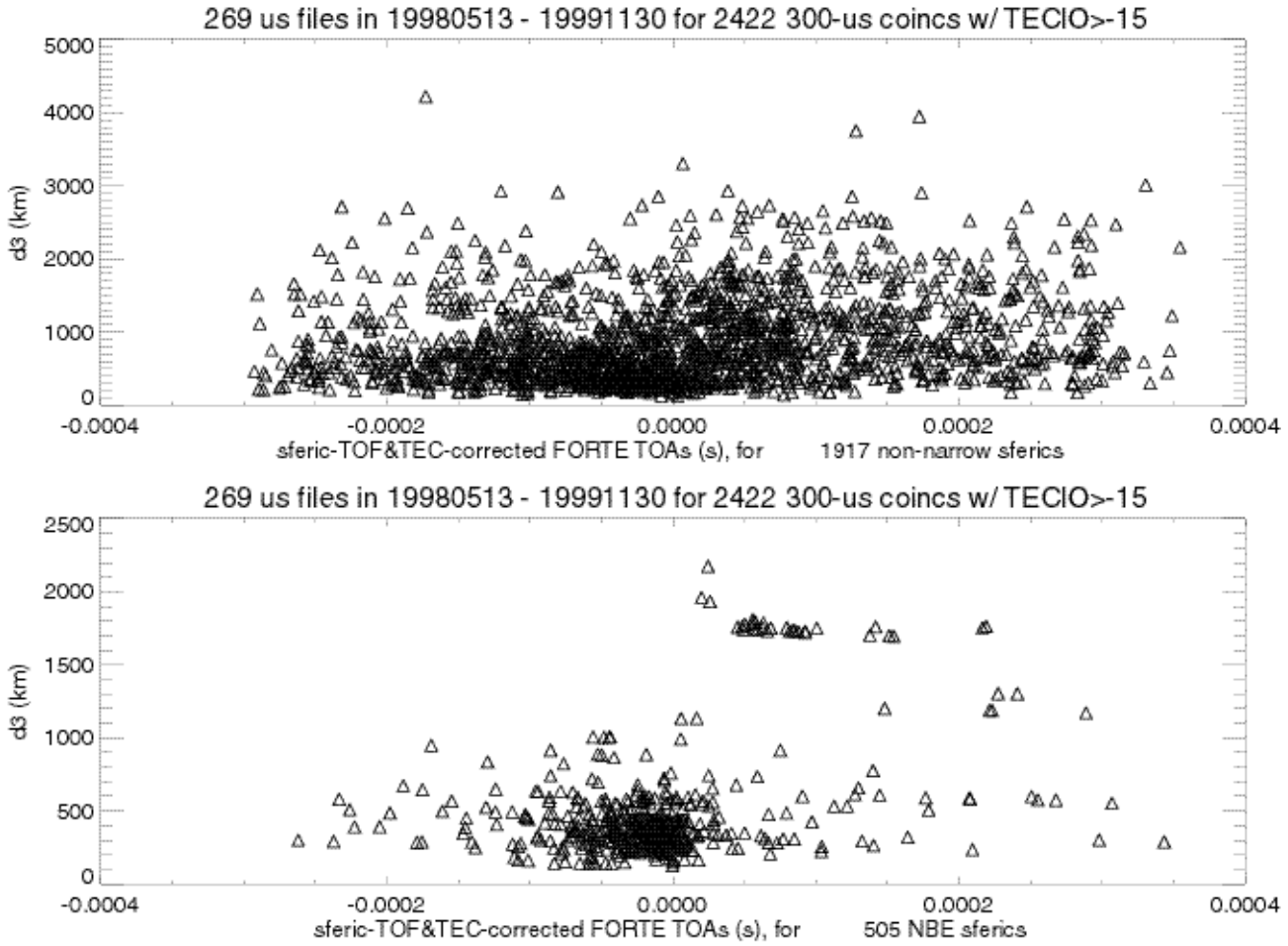

ERP vs sferic-VHF source time, for (top panel) 1917 ordinary (non-NBE) sferics, and for (bottom panel) 505 NBEs. There is no obvious narrowing of the NBE distribution at high power.

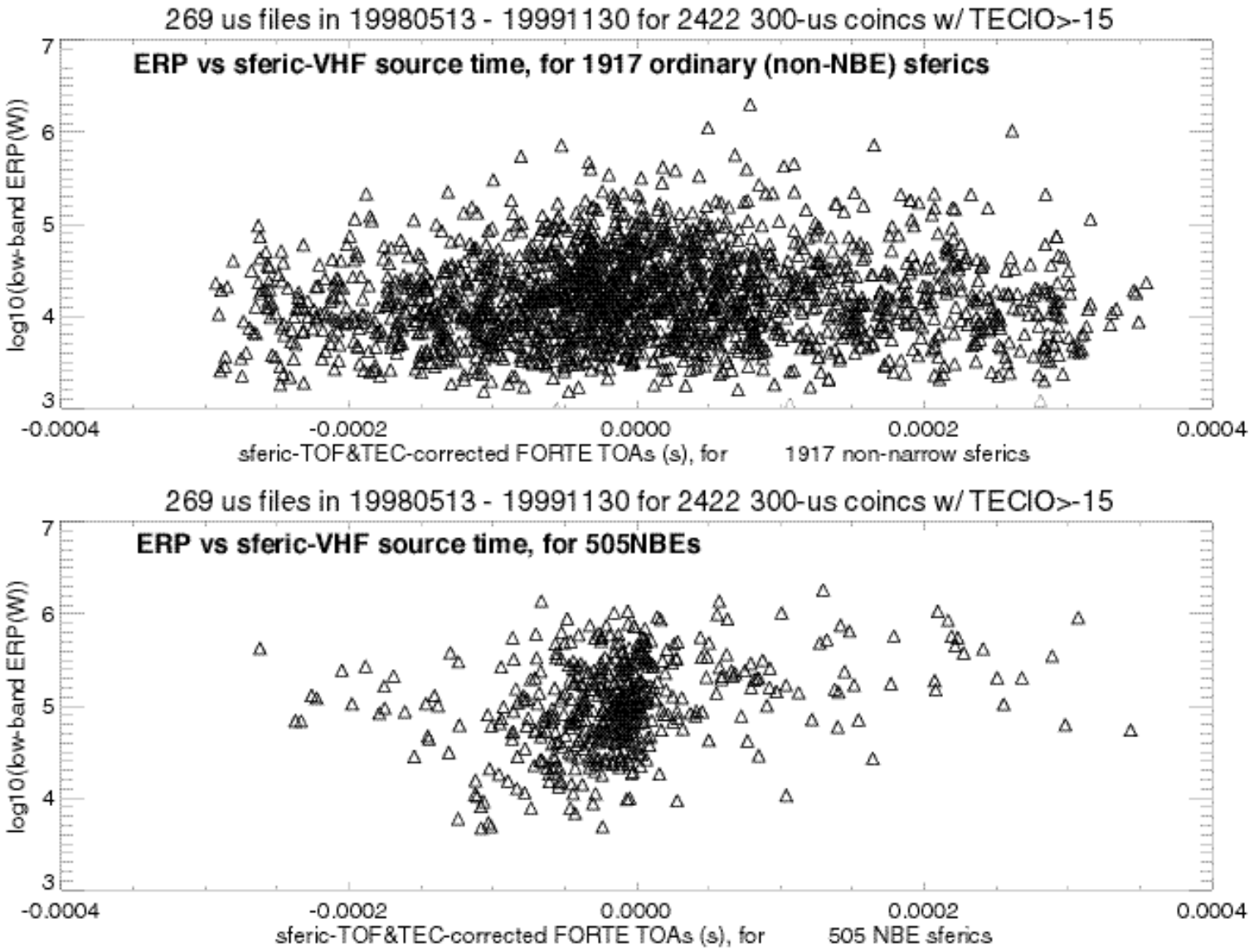

Inferred sferic-emission height versus the inferred VHF emission height, using the delay of the second pulse, which is a ground reflection. The main cluster's data lie 1 or 2 km above the equality line, as if the sferic were effectively emitted from a bit higher than is the VHF TIPP. We cannot rule out a methodological origin of this effect.

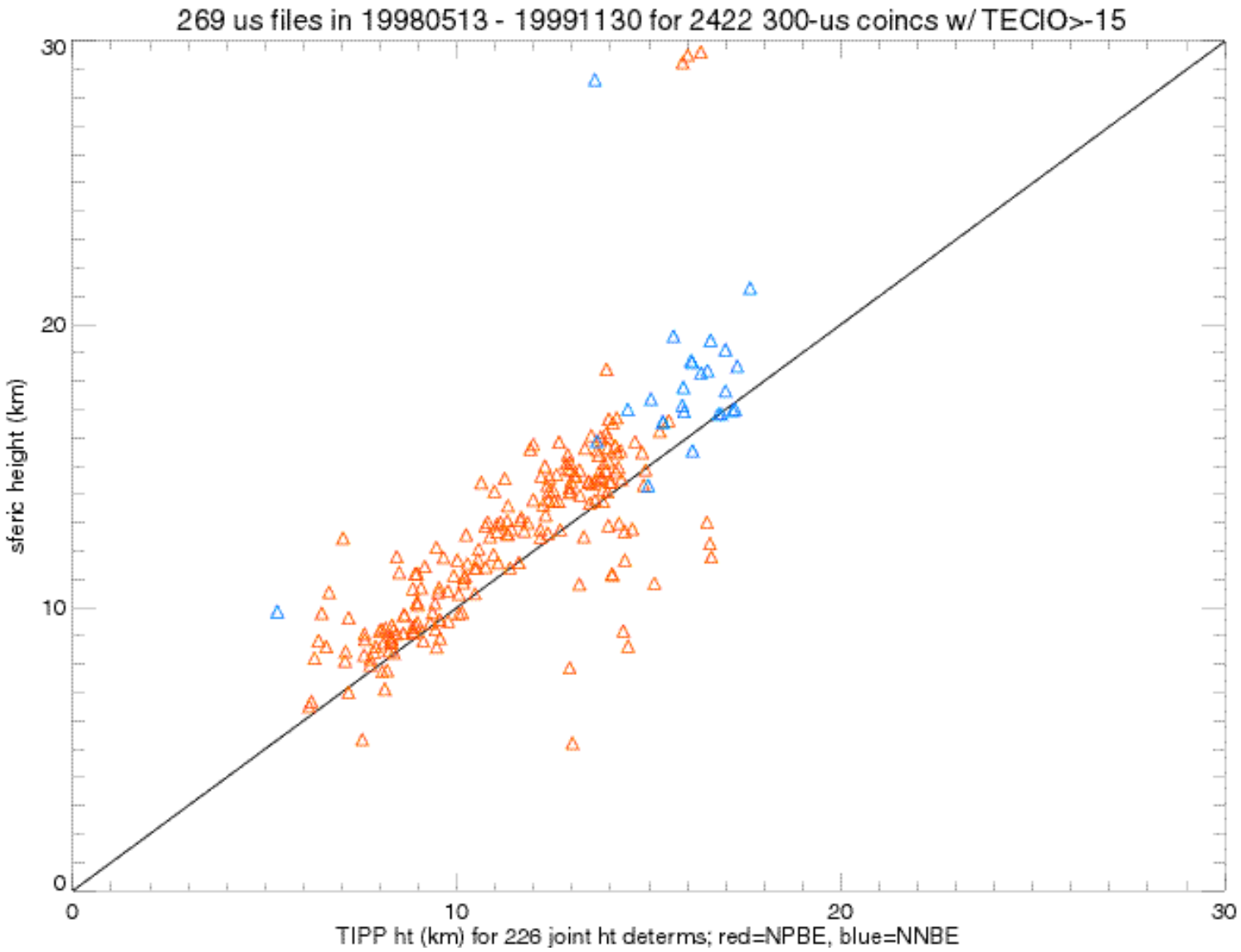

Of the FORTE VHF events that are within ± 300 μs of a sferic, we show here the probability of there being another VHF event near the sferic-coincident VHF event. This is done as a function of time difference between the VHF neighbor and the sferic-coincident VHF event. The time difference is from -2 to +2 s in bins of 0.1 s. The counts have been normalized by the number of VHF coincidences with “regular sferics” and with NBEs, so what is displayed here is true probability of a neighboring VHF event’s occuring in a given delay bin. The data show that NBE-coincident VHF events are isolated from other VHF events, relative to regular-sferic-coincident VHF events.

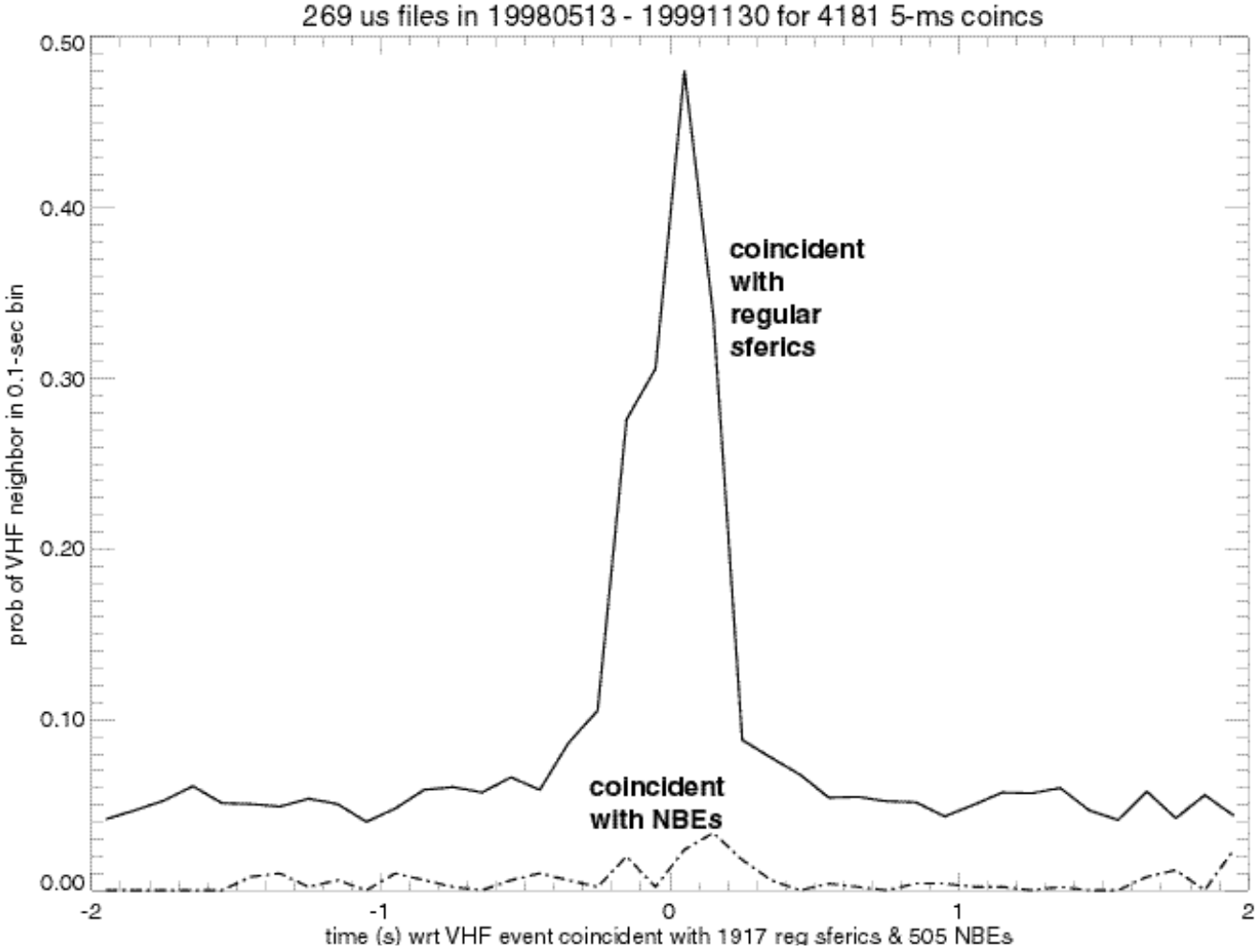

Similar to previous figure, but for a narrower time window and smaller binsize. The time difference is from -0.2 to +0.2 s in bins of 0.01 s. The counts have been normalized by the number of VHF coincidences with "regular sferics" and with NBEs, so what is displayed here is true probability of a neighboring VHF event. The data show that NBE-coincident VHF events are isolated from other VHF events, relative to regular-sferic-coincident VHF events. It is also apparent that on the timescale of a flash (~0.2 s), the VHF neighbors are more numerous after, rather than before, the key VHF event which is sferic-coincident.

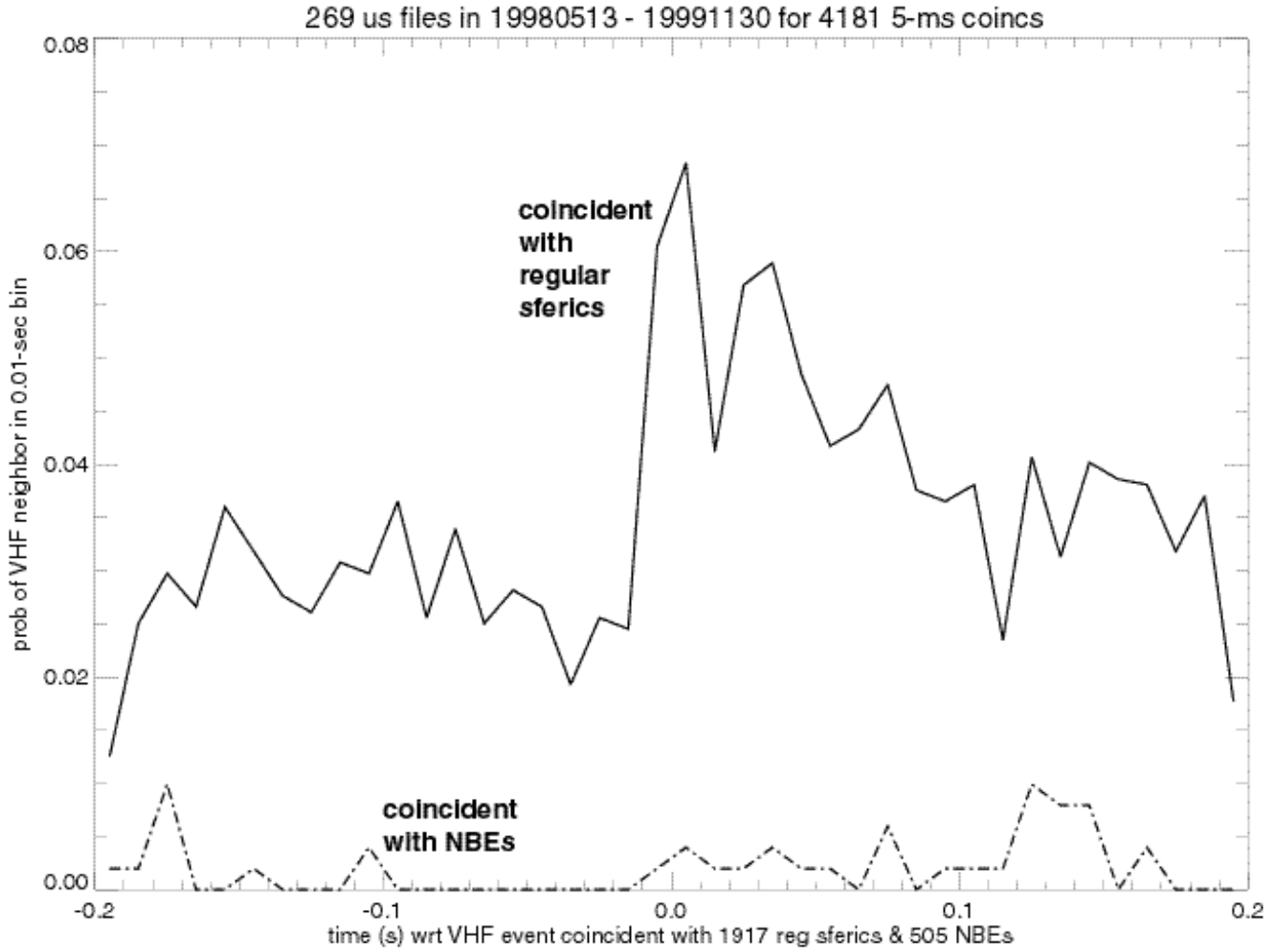

Similar to previous figure, but for a still narrower time window and still smaller binsize. The time difference is from -0.02 to +0.02 s in bins of 0.01 s. The counts have been normalized by the number of VHF coincidences with “regular sferics” and with NBEs, so what is displayed here is true probability of a neighboring VHF event. The data show that NBE-coincident VHF events are isolated from other VHF events, relative to regular-sferic-coincident VHF events. It is also apparent that in this close-in timescale (0.02 s), the most probable VHF neighbor is the one occuring within a couple of millisec of the key VHF event.